



Assessment of the reuse of Covid-19 healthy personal protective materials in enhancing geotechnical properties of Najran's soil for road construction: Numerical and experimental study



Gamil M.S. Abdullah ^a, Ahmed Abd El Aal ^{a,b,*}

^a Civil Engineering Department, College of Engineering, Najran University, Kingdom of Saudi Arabia

^b Geology Department, Faculty of Science, Al-Azhar University, (Assiut Branch), Assiut, Egypt

ARTICLE INFO

Handling editor: Zhen Leng

Keywords:

Covid-19
Waste management
Healthy personal protective materials
Geotechnical properties
Numerical simulation
Kingdom of Saudi Arabia

ABSTRACT

The COVID-19 pandemic has not only caused a global health crisis, but it has also had significant environmental and human consequences. During the COVID-19 pandemic, this study focused on emerging challenges in managing healthy personal protective materials (HPPM) in Kingdom of Saudi Arabia, using silty sand (SM) soil as an example since it covers large areas in KSA and in the whole world. The main objective of this paper is to find a novel way to minimize pandemic-related waste by using HPPM as waste materials in road construction. For the first time, a series of experiments was conducted on a mixture of different percentages of shredded HPPM (0, 0.5, 1 and 2%) added to the silty sand (SM) soil for road applications, including soil classification according to the USCS, modified compaction, UCS, UPV, and CBR. In addition, a numerical simulation was performed using geotechnical-based software Plaxis 3D to study the performance of the soil-HPPM mix as a subbase layer in the paving structure under heavy traffic loading. The modified compaction test results show that there is an increase in the optimum moisture content with increasing the HPPM contents from 0.5% to 1% and 2%. However, a reduction in the maximum dry density is observed. The values of dry density and water content at 0%, 0.5%, 1% and 2% of HPPM are 2.045, 1.98, 1.86 and 1.8 g/cm³ and 7.65%, 8%, 8.5% and 9.5%, respectively. The soaked CBR values at 0, 0.5, 1 and 2% HPPM are 23, 30, 8, 2% with the maximum value attained with the addition of 0.5% HPPM. The results of UCS were with the same percentages of HPPM 430, 450, 430 and 415 kPa, respectively, with the maximum value attained with 0.5% HPPM addition as well. In contrast, the values of UPV at 0%, 0.5%, 1% and 2% are 978.5, 680.3, 489.4 and 323.6 m/s, respectively, confirming the trends obtained by modified compaction test results. The simulation results confirm this conclusion that the soil-HPPM mix show a superior performance when used as a subbase layer and reduced vertical displacement by a percentage of 11% compared to the normal subbase material. By eliminating HPPM especially facemasks from the landfill lifecycle, incorporating them into high quality construction material production has the potential to deliver significant environmental benefits.

1. Introduction

Conservationists have cautioned that the current global pandemic caused by COVID-19, which is expected to persist through the majority of 2020, could trigger a resurgence of already-existing environmental pollution problems (Boroujeni et al., 2021). Divers have recently discovered large amounts of pandemic waste floating under the ocean's surface, including latex gloves, single-use face masks, and hand sanitizer

bottles (Roberts et al., 2020). Face masks can help prevent the spread of COVID-19; however, they can have serious environmental consequences. The environmental effects are only set to get worse as the majority of masks end up in the streets or landfills, despite the World Health Organization (WHO) adopting such guidelines during the pandemic, including the use of safe personal protective materials (HPPM) such as face coverings (Saberian et al., 2021; Sangkham, 2020). The use of HPPM by the general public will not only help prevent the

Abbreviations: HPPM Healthy personal protective materials, SM Silty sand; USCS Unified soil classification system, UCS Unconfined compression strength; UPV Ultrasonic plus wave, CBR California bearing ratio; SEM Scanning electron microscope, XRD X-ray diffraction.

* Corresponding author. Prof of soil mechanic and engineering geology Najran university, Kingdom of Saudi Arabia.

E-mail address: Ahmed_aka80@yahoo.com (A.A. El Aal).

<https://doi.org/10.1016/j.jclepro.2021.128772>

Received 2 May 2021; Received in revised form 23 July 2021; Accepted 21 August 2021

Available online 25 August 2021

0959-6526/© 2021 Elsevier Ltd. All rights reserved.

spread of COVID-19, but also has serious environmental consequences. More than (5336–38426 million pieces) of face mask are used daily in Saudi Arabia (Nzediegwu and Chang, 2020; Rowan and Laffey, 2020; Sangkham, 2020). The most widely used HPPMs are made of plastic polypropylene (Henneberry, 2020), with thousands washing up on beaches around the world long before WHO guidelines were issued (Roberts et al., 2020). Therefore, civil engineering consumes a significant quantity of natural resources. Furthermore, extraction of virgin materials produces significant amounts of greenhouse gas emissions (Saberian et al., 2019a). Moreover, compared to other waste generators, the construction industry is responsible for a substantial amount of waste (almost half of all waste generated globally), which is primarily generated by demolish buildings and other infrastructure projects (AzariJafari et al., 2016; Saberian and Li, 2019; Kazemi et al., 2020; Hajforoush et al., 2019). The main form of plastic used in HPPM, polypropylene is a thermoplastic polymer that takes more than 25 years to degrade in landfill (Thomas, 2012); however, when HPPM ends up in our rivers, they are converted into microplastics, which infiltrate our fragile habitats and potentially end up in our food supplies (Mavrokefalidis, 2020). Consequently, the impacts of global pandemic have a significant impact on the economy, and they will continue to affect our daily lives even after the pandemic is over.

Fibers have been widely used in geotechnical field to improve the geotechnical properties of soils and provide several sustainability advantages. The reinforcement of soft soils using synthetic fibers, such as polypropylene (PP-fiber), polyvinyl alcohol (PVA), and natural fibers such as coir, jute, and palm has found to enhance their strength and mechanical behavior (Tang et al., 2007; Wu et al., 2014; Sudhakaran et al., 2018; Qu and Zhu, 2021).

According to Satyam and Nisheet (2018), when the soil is mixed with 0.5 percent fibers (PPF), the specific gravity of the soil increases by 0.3%. Soil strength is related to specific gravity; the higher the specific gravity, the greater the soil strength. The plastic limit of the soil decreases in the same way that the liquid limit decreases. It drops from 29.35% to 25.8%. This result reveals an increase in shear strength, cohesiveness, and consistency of soil mass.

Al Adili et al., 2012, Gray and Ohashi (1983) performed a series of direct shear tests on dry sands reinforced with various synthetic, natural, and metallic fibers to determine the effect of several factors on shear strength, including fiber orientation, fiber content, fiber area ratios, and fiber stiffness. Gray and Ohashi determined that the increase in shear strength is directly proportional to the fiber area ratio based on the test findings. The shear strength envelopes for fiber-reinforced sand revealed a threshold confinement stress under which the fibers attempt to slip or retract. Maher and Gray (1990) performed triaxial compression tests on sand reinforced with discrete and randomly distributed fibers to investigate how different fiber qualities, soil parameters, and other test variables affected the behavior of the soil. Maher and Ho (1994) used a variety of unconfined compression, splitting tension, and three-point bending experiments to assess the mechanical properties of a kaolinite-fiber soil composite. Wahab et al. (1997) carried out extensive research to determine the impact of individual polypropylene fibers on the soil's total and effective strength parameters. Rao and Balan (2000) used coir fibers to conduct triaxial compression experiments with various fiber contents.

The application of waste materials in roads construction materials has been reported in the literature. Leng et al. (2018) using polyethylene terephthalate (PET) derived products as a performance-enhancing additive for asphalt could be one alternative for recycling and reusing this waste material. Zhang et al. (2020) used recycling construction and demolition wastes (CDW) in subgrade materials, which is a promising method to process these wastes, with significant environmental and economic benefits. Zhange et al. (2021) also investigated the performance of cement stabilized recycled mixture containing recycled concrete aggregate (RCA) and crushed brick (RCB), for highways applications. Moreover, Zhange et al. (2021) conducted a series of

laboratory tests to study the variation law of the dynamic resilient modulus of recycling construction and demolition (C&D) waste, used as fillers in pavement subgrade, under repeated freeze-thaw cycles and establish a reasonable performance prediction model. Abdullah and Al-Abdul Wahhab (2015), (2019) studied the performance of foamed and emulsified asphalt modified with 30% sulfur for roads application.

The rationale for using masks for soil improvement is the material that mask made of which called meltdown polypropylene that is considered a good material for soil improvement since it acts as a reinforcement. In addition, face masks materials are non-biodegradable plastics, which means that they take hundreds of years to degrade in the environment causing problems for wildlife or killing animals and marine life. Therefore, using these waste materials in soil improvement and reducing the environmental risks associated with its disposal is a noble task.

The main objective of this research is to investigate whether disposal face masks can be recycled and reused in order to reduce the amount of pandemic-related waste that ends up in landfills or litter the streets during this current crisis. Through a series of experiments, the effects of COVID-19 HPPM polypropylene fibers from on the geotechnical properties of Najran soil were evaluated as an example in KSA.

Due to the increase in littering, used face masks can be found almost everywhere, from city streets to car parks to local parks. Because of the lightweight design of masks, wind and rainwater can easily transfer to city streets, rivers, and oceans, where the plastic-based masks can be broken down into microplastics. As a result, discarding masks or poor waste disposal of used personal protective equipment will result in wildlife problems or death of animals and marine life (Prata et al., 2019; Fadare and Okoffo, 2020 Prata et al., 2020 and; Hale and Song, 2020). Pandemic-related waste by recycling and repurposing HPPM (SFM) and mixing it with the sandy soil for road construction subbase. A series of tests, including a modified compaction test, an unconfined compression strength test, and a CBR, were conducted for the first time to assess the feasibility of using HPPM as a road subbase material. The findings of the current study can be used to provide practical advice on how to apply HPPM. The novelty of the current research lies in the first attempt to use polypropylene fibers obtained from HPPM in soil improvement.

1.1. Regular facemask usage estimates in KSA with confirmed COVID-19 cases

Face masks are the first line of protection against the coronavirus 2 that causes extreme acute respiratory syndrome (SARS-CoV-2). The World Health Organization (WHO) has also revised its recommendations, recommending the use of face masks in public places.

For critical service personnel (e.g., physicians, nurses, caregivers, prepares, etc.) and others treating COVID-19-infected patients, the use of safe personal protective martials (HPPM) such as medical caught, facemasks, and aprons has been suggested. Facemasks are becoming increasingly common in public places in a growing number of countries. As a result of these recommendations, millions of HPPM are made and used on a regular basis during the pandemic. The amount of HPPM (e.g., facemasks, suites and overhead) used on a regular basis in Saudi Arabia is estimated to be in the hundreds of millions, with COVID-19 cases mandating mandatory facemask use for their people (WHO, 2020a, b). The following equation can be used to measure total regular facemasks:

The total number of masks to be used in Saudi Arabia (per year) is calculated using the total population (P), the percentage of urban population (c), the mask acceptance rate (d), and the average daily number of masks (b) used per person. $DMU = P * c * d * b$ (Nzediegwu and Chang, 2020). Annual mask consumption (AMU) is calculated using the formula $AMU = DMU \times 365$. In this analysis, we looked at various levels of d and b for different acceptance rates, such as d = 0.5, 0.6, 0.7, 0.8, and 0.9, and b = 1, 2, 3, and 4. For each combination of d and b, the AMU is calculated.

Saudi Arabia is expected to have the largest number of face masks

(5336–38426 million) and polypropylene/(micro-) plastic material (32.69–235.36 thousand tons). This is because plastic particles can serve as a potential carrier of pathogenic microorganisms such as viruses, bacteria, and fungi is gaining traction (Jiang, 2018; Neto et al., 2019).

2. Research methodology

This research aims to study the reuse of healthy personal protective materials (HPPM) such as face masks, head and feet safety covers, and body protective suit in enhancing the geotechnical engineering properties of Najran soils for road construction. The methodology utilized to achieve this goal consists of four stages: (i) the collection and characterization of materials; (ii) conducting experimental laboratory work; (iii) analyzing the laboratory tests results and comparing the findings with the indigenous soils; (iv) performing a numerical analysis to predict the performance of HPPM-soil mixes in the pavement structure (v) studying the environmental impacts.

3. Experimental work

3.1. Materials

It is well known that the use of used healthy personal protective materials (HPPM) in any experimental work without any precautions and careful manipulation, especially during the COVID-19 pandemic, is not permitted, and is in contravention of the current laboratories workplace safety regulations and limitations. Therefore, clean and new HPPM were used in the study in which they were shredded to arbitrary shape and size not exceeding a width of 0.5 cm and a length of 2 cm. Before using HPPM, all accessories such as gear loops, the metal strip of masks and thread used for closing the protective suits were taken out. The face masks consist of three layers in which the top and bottom layers are made of non-woven fabric, while the middle layer is made of melt-down polypropylene. For the head, feet, protective and body jacket materials are made of polypropylene fibers. X-ray diffraction and scanning electron microscope (SEM) tests were conducted on HPPM samples and the results will be discussed in the Results and Discussion part.

Soil samples from Najran city were collected, dried, characterized and then stored in plastic drums for use in this research as a compacted subgrade layer or subbase layer in roads construction. The soil is mixed with three different percentages of HPPM (0.5, 1 and 2%) by weight of soil. The basis for selecting the dosage of HPPM is based on many criteria including literature review of using polypropylene and fiber ranging from 0 to 5% (by weight% of soils) (Yaghoubi et al., 2017; Mishra and Gupta, 2018) in enhancing concrete and soils properties and the light weight of masks material compared to soil. Tests results on these mixtures were compared with the reference soil (0% of HPPM).

3.2. Tests and methods

To determine the basic characterization, physical and engineering properties of the parent soil, many tests were conducted such as specific gravity (ASTM D 854), sieve analysis (ASTM D 422) and Atterberg limits (ASTM D4318-17e1 and ASTM D 424). Moreover, x-ray diffraction was conducted on soil sample to obtain its minerals and chemical composition. The Modified Proctor compaction (ASTM D 1557), Ultrasonic pulse velocity (UPV), unconfined compressive strength (ASTM D 2166) and California bearing ratio (CBR) (ASTM D 1883) tests were conducted on soil-HPPM mixes as well as on the parent soil (0% of HPPM). For HPPM, their physical properties, such as tensile strength test, water absorption, melting point, and specific gravity, have been reported in the literature (Saberian et al., 2021).

The optimum moisture and dry density values of the suggested mixtures were determined, as well as the calculation of the unconfined compressive strength 'UCS' and the soaked California Bearing Ratio (soaked CBR) for the prepared soil-HPPM mixtures meeting the

necessary strength limits.

3.2.1. Ultrasonic pulse velocity (UPV)

In order to find out the homogeneity and integrity of the structure of produced soil with HPPM, ultrasonic pulse velocity (UPV) tests were conducted according to ASTM C597. The velocities of the longitudinal waves were determined using the pulse transmission method, which consists of coupling two piezoelectric sensors on the opposite faces of the sample with a diameter of 60 mm and a length of around 120 mm. The velocity of the ultrasonic waves was measured with a commercially available meter (Matest Company). A viscoelastic gel was applied on flat surface of the sample. The sample was placed between the transmitter and the receiver and the faces of the transducers were firmly pressed against the face of the rock samples until a stable velocity is displayed. The pulse transmission technique is used to measure the UPV using Panametrics Pulser-Receiver (Model 5058 PR) and an Agilent DSO-X-2014A Digital Storage Oscilloscope (100 MHz) (ASTM, 2008a).

3.2.2. Unconfined compressive strength (UCS)

The unconfined compressive strength was calculated using the procedures outlined in ASTM D 2166 (2016). The treated soil samples were blended and compacted at the optimal moisture content after being mixed for 5 min in a geomechanical mixer. The mixture was then pressed in three layers into a mold of 6 cm in diameter and 12 cm in height (H/D = 2) to a maximum dry density. To avoid segregation, the methods recommended by Yaghoubi et al. (2017) were followed, so that the mixed materials were poured into the mold for each layer by keeping the scoop very close to the top layer of the sample inside the mold. After compaction, specimens were chipped and covered with three layers of plastic sheets to prevent moisture from evaporating. The wrapped specimens were cured for 7 day at room temperature ($22 \pm 3^\circ\text{C}$) before being checked for unconfined compressive strength (UCS). According to ASTM D559M-15 (2015), 7 days are expected to achieve the optimal time for soil strength.

3.2.3. California bearing ratio (CBR) test

California bearing ratio (CBR) test was originally developed in California, USA, as a means of evaluating the suitability of soil for use as a sub-grade material in pavements and subsequently it was adapted by the engineering communities as an empirical test to measure the strength of soil under controlled moisture and density conditions. The test is globally recognized due to its simplicity and applicability. Therefore, the test can easily be used to quantify the material for use in pavement construction.

In this investigation, soaked CBR tests were conducted in compliance with ASTM D 1883. The CBR mold has a height of 5 in (127 mm) and a diameter of 6 in (152 mm). The mixtures were mixed at the optimum moisture content and compacted in the CBR mold in 5 layers and the number of blows per layer was 56 to satisfy the compaction energy requirement. Since the ground water table is relatively close to the ground surface for the majority of the soils in the region, the prepared specimens were subjected to a surcharge load of 4.5 kg and submerged in water for 96 h before testing to simulate actual field conditions and the potential for swelling is monitoring during soaking.

To depict a clear picture about the conducted laboratory work, Fig. 1 summarizes the experimental program of this study.

4. Results and discussion

4.1. Soil geotechnical characterization results

The basic geotechnical characterization of the soil used in this research was obtained through a set of geotechnical tests such as specific gravity, Atterberg limits and sieve analysis. The specific gravity test result shows that the soil has a value of 2.67. In contrast, Atterberg test results show that the soil is non-plastic in which we cannot be rolled to a



Fig. 1. Tests and methods in the present study.

thread with a diameter of 3.18 mm and cannot get the number of blows for the liquid limit. **Fig. 2** presents the sieve analysis results. From the figure, it can be seen that the percent of sieve passing No.200 is 2.3%, and the soils are classified as silty sand "SM" in accordance with USCS and A-3 in as well as AASHTO soil classification systems.

4.2. Physical properties of HPPM

Fig. 3a shows the integrated X-ray diffraction patterns of the fibres. The diffraction peaks of all fibers were obtained between 10 and 30°, as shown in the figure. The peaks obtained at approximately 14°, 17°, 18.6°, 21–22°, and 28° are similar to the peaks generated by -polypropylene ([JCPDS 00-050-2397- 1970](#)). The SEM of HPPM is shown in

Fig. 3b and the polypropylene fibers are clearly shown.

With regard to the HPPM, **Table 1** presents their physical properties such as water absorption, tensile strength test, specific gravity and melting point (Saberian et al., 2021). It is worth mentioning that head cover, feet cover, and body jacket materials are the same as materials of face mask, and they have the same physical properties.

4.3. Modified proctor compaction test results

The results of the modified Proctor compaction test conducted on triplicate specimens of the parent soil and the soil mixed with various percentages of HPPM (0%, 0.5%, 1% and 2%) are shown in **Fig. 4**. Results were presented in terms of change in the water contents with unit

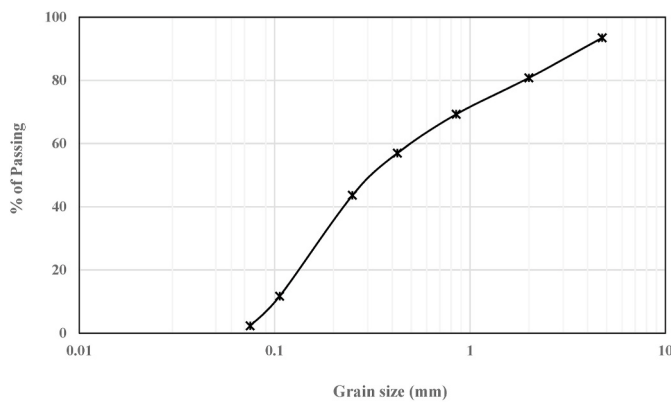


Fig. 2. Soil grain size distribution.

dry weight. The results showed that there was an increase in the optimum moisture content as the HPPM contents increased from 0.5% to 1% and 2%. However, a reduction in the maximum dry density was observed. This trend is clearly demonstrated in Fig. 5. The dry density decreased from 2.045 g/cm^3 for parent soil (0% HPPM) to 1.98 , 1.86 and 1.8 g/cm^3 when the 0.5, 1 and 2% of HPPM were added to the soil, respectively. In contrast, the water content increased from 7.65% for the parent soil (0% of HPPM) to 8, 8.5 and 9.5% with increasing HPPM as well as 0.5, 1 and 2%, respectively. The reduction in the maximum dry density is ascribed to the lower specific gravity value of the HPPM compared to that of the parent soil. This method is similar to that obtained by Yaghoubi et al. (2017) and Perera et al. (2019) when they added polyethylene terephthalate, low-density polyethylene, and high-density polyethylene to the aggregates. A comparable tendency was also detected by Siberian et al. (2021) regarding the addition of a shredded facemask (SFM) to recycled concrete aggregate (RCA).

4.4. Ultrasonic pulse velocity (UPV)

Ultrasonic testers are inexpensive and easy to use. They are also transportable and can be used in the field. If there are clear correlations between P-wave velocity and UCS, ultrasonic measurement can be used to quickly estimate UCS and many other engineering properties during the preliminary investigation project (Fener et al., 2005).

To assess the trend of decreasing dry density with the increase in HPPM percentages, nondestructive test ultrasonic pulse velocity (UPV) was measured on a sample prepared for parent soil (0% of HPPM) and soil blended with different percentages of HPPM (0.5%, 1% and 2%) and the results are depicted in Fig. 6 a, b. Results in the figure show a decrease in the UPV with the increase in the HPPM percentage,

indicating an increase in the porosity or voids of the samples due to the inclusion of HPPM with higher percent, which in turn means a lower density. This is in consistent of the findings obtained by modified Proctor compaction tests. P wave velocities calculated with undisturbed samples of various soil types were associated with soil properties, and regression analysis was used to construct prediction equations (Fig. 6 c).

Table 1
Physical properties of HPPM (Saberian et al., 2021).

Physical properties	Shredded Face Mask (SFM)
Specific gravity	0.91
Melting point ($^{\circ}\text{C}$)	160
Water absorption 24 h (%)	8.9
Tensile strength (MPa)	4.25
Tensile strength at break (MPa)	3.97
Elongation at break (%)	118.9
Rupture force (N)	19.46
Aspect ratio 24	24

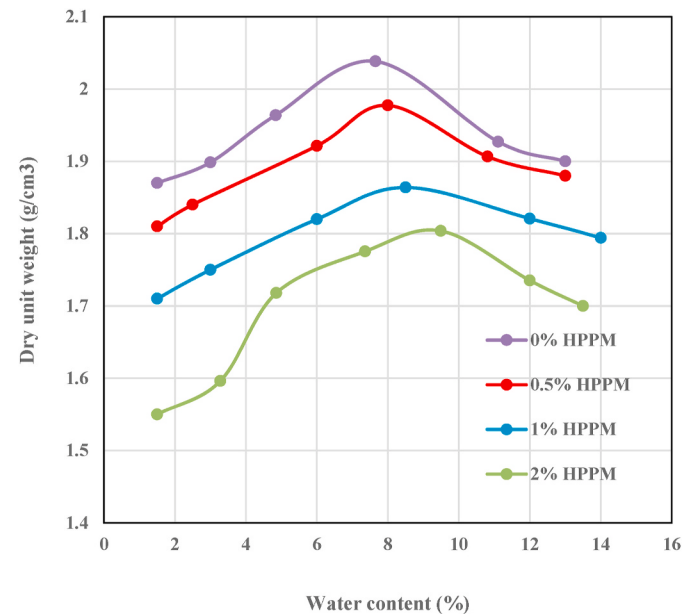


Fig. 4. Relationship between moisture content and dry density of soil-HPPM mixes.

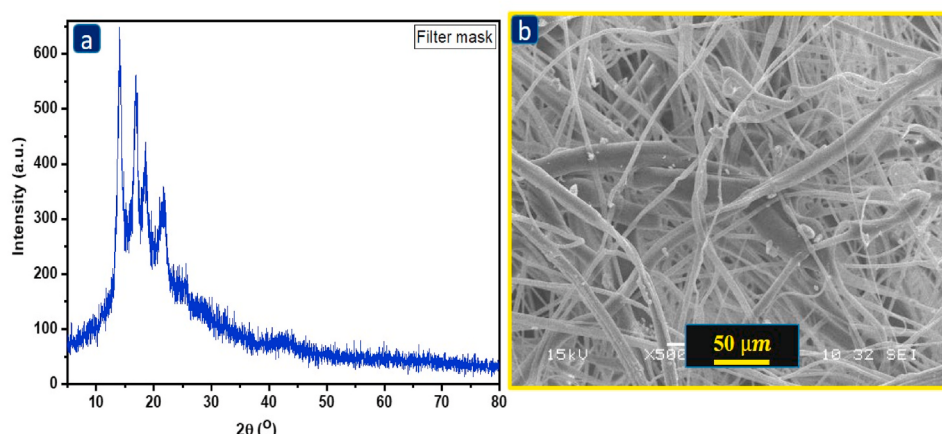


Fig. 3. Microstructure of HPPM a) XRD patterns of cross-sectional shaped polypropylene fibers b) SEM.

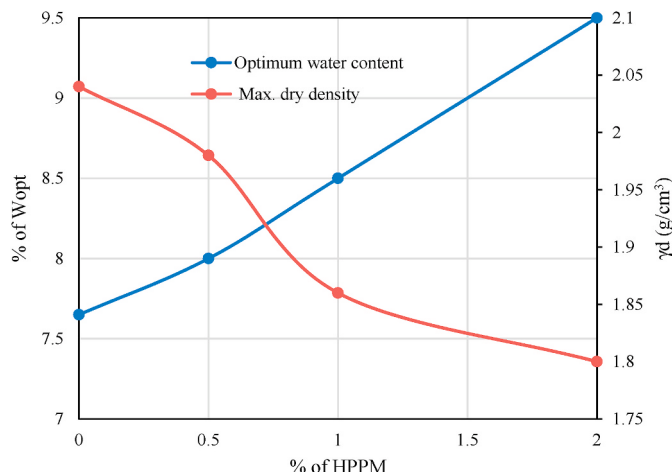


Fig. 5. Effect of addition HPPM on the optimum moisture content and maximum dry density.

4.5. California bearing ratio (CBR) test results

For materials used as a subgrade or subbase layer in a pavement structure, it is very important to obtain California bearing ratio (CBR) values to examine their performance under traffic loading. To simulate the worst conditions in the field, soaked CBR tests were conducted on the soil samples mixed with various percentages of HPPM. The tests were triplicate, and the average is presented in Fig. 7. It is clear from the figure that there is an increase in the CBR value from 23% of the parent soil to 30% when 0.5% of HPPM is added. Then, a dramatic decline in the CBR value was noticed when the percent of HPPM increased to 1%, in which CBR decreased from 30% to 8%. The percentage reduction in CBR value is almost 73%. Moreover, the decrease in the CBR value continues significantly with the increase in the HPPM percentage as it decreased from 8% to 3% when HPPM addition increased from 1% to 2%. This can be attributed to the increase in water absorption during the soaking period with the increase of HPPM percentage which led to a decrease in the strength and hence lower CBR values. It is worth mentioning that swelling was monitored and measured during the

soaking period, and the results indicated that there is no swelling occurred in the soaked CBR samples. It can be concluded that the addition of 0.5% of HPPM gave the highest value of soaked CBR value and it can be used as a subbase layer in the structure of heavy traffic loading roads as per specifications. This strength is gained by the action of reinforcement introduced by 0.5% HPPM in the soil structure as shown in Fig. 8. As can be seen, the shredded HPPM comprises a bridge under the CBR machine-loading plunger and since its percentage is low (0.5%), therefore the water absorption is low as well which enhanced the resistance of soil-HPPM mixture to the penetration and gave a higher CBR value (30%).

It should be noted that, CBR tests were done on specimens after they were soaked in water for 4 days (i.e. soaked CBR tests) so that they are considered saturated and thus the unsaturation effects are ignored.

4.6. Unconfined compression strength test results

To evaluate the pavement materials in term of strength, unconfined compressive strength test should be conducted (MolaAbasi et al., 2019). Therefore, Fig. 9 depicts the results of the unconfined compressive strength test for soil mixed with various percentages of HPPM (0.5%, 1% and 2%) compared to the reference soil (0% of HPPM). Tests were

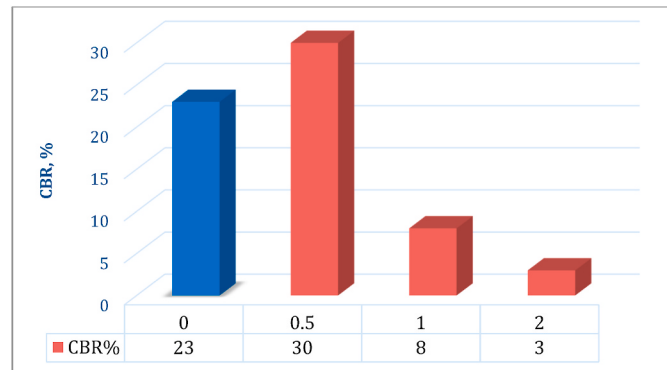


Fig. 7. Effect of addition HPPM on the soaked CBR value.

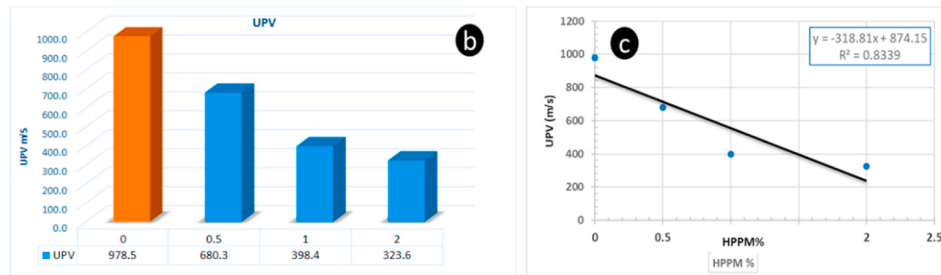


Fig. 6. Effects of the addition of HPPM on Ultrasonic pulse velocity, a) Ultrasonic pulse velocity test, b) Ultrasonic pulse velocity results, c) The relationship between UPV and HPPM percentage.

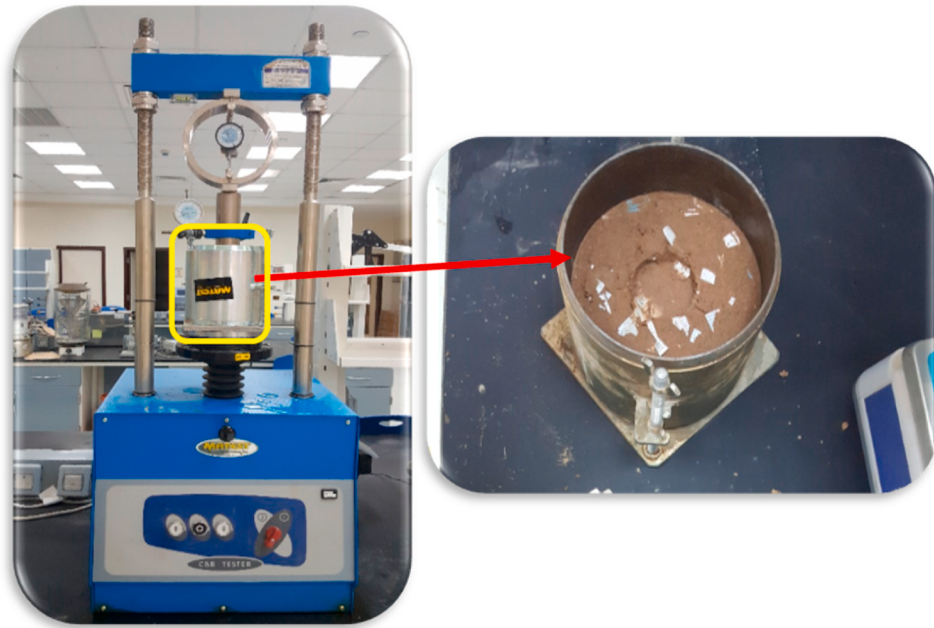


Fig. 8. Bridge and reinforcement action of the inclusion of 0.5% of HPPM in Soaked CBR.

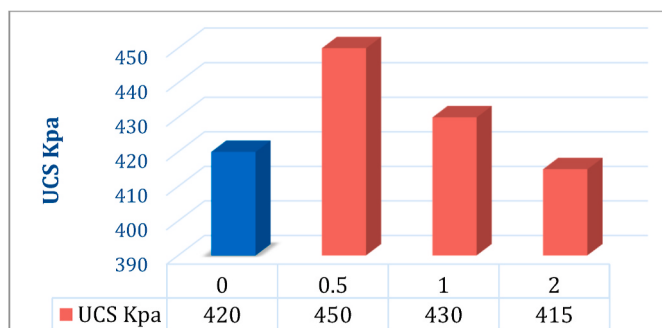


Fig. 9. Effect of HPPM addition on UCS.

triplicate, and the average is presented. The results showed an increase in the UCS with the addition of 0.5% of HPPM as UCS increased from 420 kPa for parent soil (0% of HPPM) to 450 kPa with an increase ratio of 7%. However, a further increase in HPPM to 1% and 2% leads to a decrease in the UCS values to 430 and 415 kPa, correspondingly. This means there is an onset value of HPPM percentage addition beyond which the unconfined compressive strength decreases. The reduction in the UCS with the increase in the HPPM percentages is attributed to the higher voids ratio due to the addition of a high percentage of HPPM and hence stiffness loss for blended specimens. When the HPPM content is higher, the HPPM is dispersed unevenly in the soil due to poor workability and mixing. As a result, these HPPM amounts gathered to form comparatively weaker points that serve as voids, making them more vulnerable to cracking, resulting in a decrease in compressive strength. A comparable tendency was obtained by Chen et al. (2015) in their study on the clay soil reinforced by polypropylene. Moreover, Saberian et al. (2021) got the same trend with the addition of shredded facemasks with RCA. Fig. 10 demonstrates the reinforcement effects of the HPPM under the UCS loading stage. The bridging action of the fibers in the soil particles may hinder the additional formation of tension cracks because the HPPM fibers provided a reinforcing function in linking the soil particles (Fig. 10 b, c). Tomar et al. (2020) and Bojnourdi et al. (2020) obtained similar findings for soil reinforced with polypropylene fibers.

In the soil testing, soils are all unsaturated. Specimens with different

HPPM content were prepared at the same water content and are expected to have different suctions due to different soil microstructures. Suction stress refers to the net interparticle force generated within a matrix of unsaturated granular particles (e.g., silt or sand) due to the combined effects of negative pore water pressure and surface tension. The macroscopic consequence of suction stress is the force that tends to pull the soil grains towards each other. Consequently, for the same water content, increasing the percentage of HPPM causes the water to be absorbed mostly by HPPM and not by the soil particles, implying reduced suction stress. This is clearly shown in the results of UCS test results as the UCS dropped from 450 kPa at 0.5% HPPM to 430 and 415 kPa at 1 and 2% HPPM, respectively.

4.7. Discussion of the trend of UPV, UCS and CBR test tests

In fact, the UPV depends on the density of the sample so that when the HPPM content increases the voids in the sample increase, which in turn leads to decreased density. Therefore, due to lower density, the UPV decreases. On the contrary, the mechanism in attaining UCS and CBR depends on the reinforcement action introduced by HPPM that acts as a bridge and enhances the strength of the mixture as seen in Figs. 8 and 10.

The inclusion of HPPM may bridge cracks created in the soil matrix. As soil microcracks appear, HPPM filling bridges the distance between the neighboring edges of the microcracks while also improving the microstructure of the soil mass. By contacting the matrix, the HPPM can reduce the crack width and area as it extends further. When the soil mass cracks, the added HPPM forms a three-dimensional platform that links cracks and transmits distributed stress. When the HPPM content is higher, the HPPM is dispersed unevenly in soil due to poor workability and mixing. As a result, these HPPM amounts aggregate to form relatively weak points that serve as voids, making them more susceptible to cracking, resulting in a decrease in density, compressive strength and CBR.

The conclusion that the optimal content of masks is 0.5% is drawn based on the percentage of mask quantity that gave higher dry density, CBR, and UCS. Based on Figs. 4, 7 and 9, it is clear that 0.5% HPPM gave the higher values for these engineering properties of treated soil.

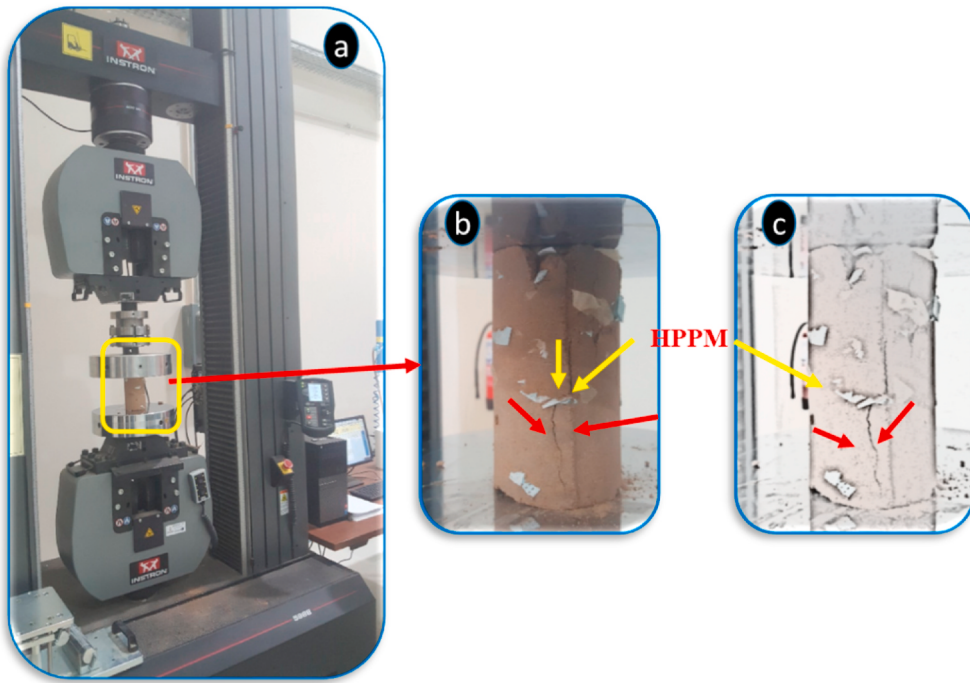


Fig. 10. a) Test instrument b) Reinforcement action of HPPM in blended samples c) bridging.

5. Finite element simulation

To predict the optimum soil mixture performance with 0.5% of HPPM according to the results of the soaked CBR and unconfined compressive strength tests, finite element modeling using Plaxis 3D geotechnical-based software is conducted. The model consists of a natural subgrade, soil-HPPM mix as a subbase (0.3 m), granular base (0.15 m) and asphaltic concrete (0.1 m) layers. Axisymmetric modeling was chosen and performed because it can simulate circular loading of the wheel trucks and does not require excessive time for computation. Due to the property of symmetry, only one quarter is simulated to reduce the time of computation. Modeling is done for both pavement structure with soil-HPPM subbase and for the structure with normal subbase layer (i.e. soil without HPPM) for comparison purposes. Fig. 11 shows the model geometry. The dimensions of the model are selected as 3, 3, and 5 m for length, width and depth, respectively, as per the criteria stated by Alex (2000). He demonstrated that the strains of nodal radial are usually anticipated to be ignored at around ten times the radius of the area of distributed loading representing utilized wheel load. Furthermore, the nodular displacements and stresses are also expected to be insignificant and ignored at twenty times the radius of the area of applied load under

the pavement surface.

Mohr-Coulomb constitutive model available in Plaxis 3D is selected to represent the nonlinear behavior of the materials in subgrade, subbase and base layer while the linear elastic model is selected for asphaltic concrete layer. The material properties for all layers are listed in Table 2. The basis for the value of each parameter is based on laboratory test results and empirical equations reported in the literature. A contact pressure of about 550 kPa was used to model the load applied to a dual wheel on the pavement structure. The tire impact pressure on the pavement is equal to the tire inflation pressure, and the tire imprint is a circular shape with a radius of 200 mm. The simulation boundary conditions are that the model is constrained to the bottom, and there are no motions in the directions vertical to the symmetry planes, which is called roller support.

Plaxis 3D automatically creates the mesh after selecting the meshing type as shown in Fig. 12. The mesh of the finite element model is created using ten node tetrahedral elements to represent all layers of the pavement structure. To obtain reliable results, the effect of mesh size is eliminated by using the fine mesh analysis for pavement structure. Around 54481 elements and 78817 nodes are created during mesh generation.

5.1. Analysis results

After the model is built and input all material properties for each

Table 2
Materials properties.

Properties	Asphalt concrete	Base	Subbase (soil + HPPM)	Natural Subgrade
Modulus of Elasticity (kN/m ²)	3.5×10^6	200000	167000	29000
Poisson's ratio (μ)	0.45	0.35	0.3	0.3
C (kN/m ²)	—	0.1	10	0.1
ϕ degree	—	30	35	35
dry unit weight (kN/m ³)	—	19	19.8	18

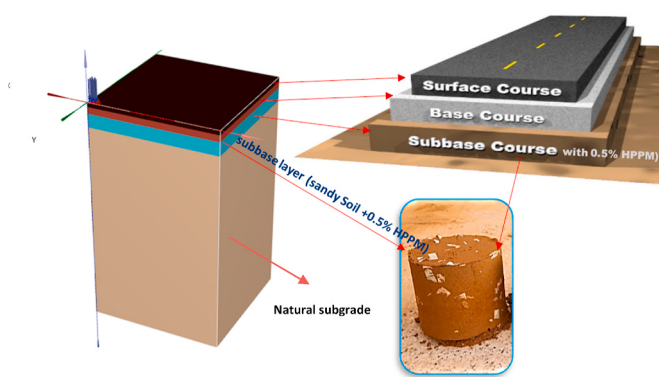


Fig. 11. Finite element model geometry.

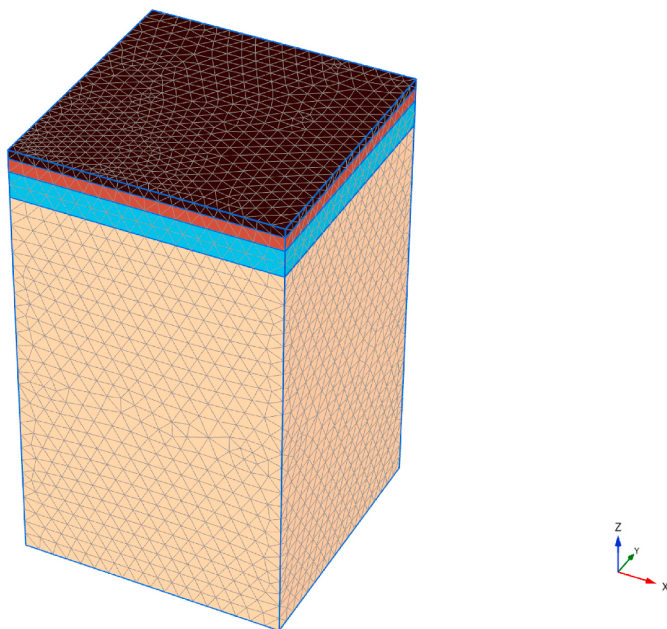


Fig. 12. Finite element generated mesh.

layer, analysis is conducted, and the results are extracted and presented. Fig. 13 shows the deformed mesh of the model after loading.

The finite element method produces an accurate analysis and estimation of stresses, forces, and displacements. For roads, it is very important to evaluate the vertical deformation of the pavement structure under traffic loading. Fig. 14 and Fig. 15 show the vertical displacement of the pavement structure with normal subbase and of the structure with soil-HPPM subbase, respectively. It is noted from the figures that there is a decrease in the total displacement of the pavement structure when the soil-HPPM mix is used as a subbase layer. The displacement decreases from a value of 2.107×10^{-3} m to 1.872×10^{-3} m with a reduction rate of about 11%. This leads to a conclusion that using HPPM has positive effects on the pavement structure performance and can reduce the rutting distress to a certain degree. Enhancing the engineering properties of the soil along with the disposal of daily healthy waste materials is essential to the safety of the environment.

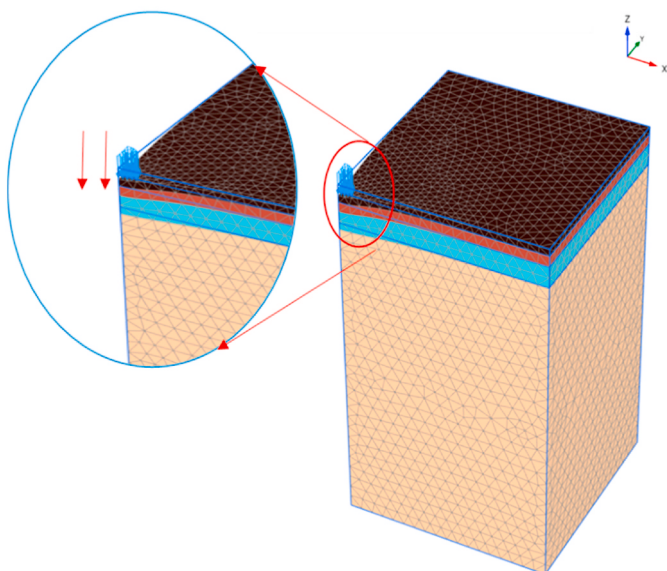


Fig. 13. Deformed mesh.

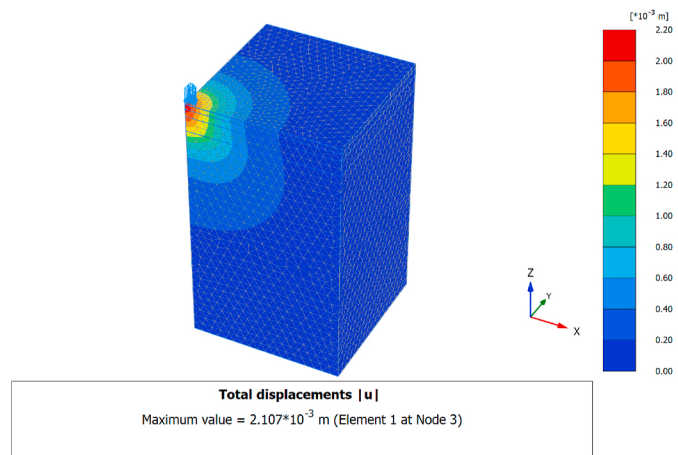


Fig. 14. Total displacement of pavement structure with the normal subbase.

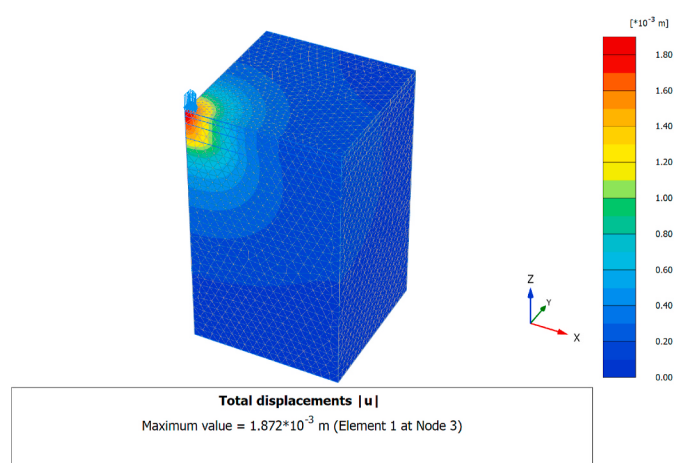


Fig. 15. Total displacement of the pavement structure with soil-HPPM subbase.

6. Environmental impact and solid management of HPPM

Millions of contaminated HPPM (e.g., mainly facemasks and suite) would end up as wastes, which if improperly managed, can pose environmental and health threats (Fig. 16), especially as a recent study (Kampf et al., 2020) found that the coronavirus can survive on material surfaces (e.g., metals, glass, and plastics) for up to 9 days. These threats may be ameliorated in developed countries where green and sustainable waste management strategies, capable of containing such viruses, are practiced. However, the threats would be much higher in developing countries that have poor waste management strategies.

Although many developing country governments are taking effective measures to contain and reduce the spread of COVID-19, strategies to manage solid wastes, including used PPE, during and after the COVID-19 pandemic, are not available. The government can adopt the strategies developed by the Lagos State Waste Management Authority, where proactive measures are taken to restrict the access of waste pickers to its landfills. Special waste collection buckets to collect disposable HPPM can be provided in buildings (residential, government and hospitals) and in public places. These waste collection buckets could be emptied, at least daily, by trained personnel who then decontaminate or dispose the HPPM following WHO 2020a, b. Used plastic bottles could be decontaminated with a 70% alcohol solution, according to NCDC guidelines, before being reuse in packaging local drinks and herbal medicines.

There are other potential pathways where improper management of used HPPM can pose a significant risk for increasing the transmission of



Fig. 16. Discarded used HPPM mainly face masks in public spaces in Victoria during the COVID-19 pandemic.

COVID-19. We thus call on the scientific community to express their concerns to governments at various levels about the need to develop proper strategies for managing solid wastes, such as used HPPM, to curb the spread of the novel coronavirus.

In fact, the masks used contain bacteria and viruses may cause pollution to groundwater, however, there are different ways and methods available for disinfecting and sterilizing the face masks for reuse or before disposing. Doan (2020) recommends the microwaved method for disinfecting disposable medical masks. In this method, an antiseptic solution (i.e., 0.9% physiological saline) should be sprayed on the masks to maintain moisture. Then, the moist masks have to be heated in a microwave oven, having a default capacity of 800 W, for about 1 min. It is worth noting that the sprayed sides of the masks have to be faced. This sanitizing method can effectively kill 99.9% of viruses (Doan, 2020). Xiang et al. (2020) reported that dry heat at both 60 °C

and 70 °C for 1 h could ensure the decontamination of a surgical face mask while maintaining filtration efficiency.

To eliminate the risk of exposure to COVID-19 virus during transportation and construction, it is suggested that face masks, after disinfection, in an open and restricted area, and exposed to the sun and air for a week prior to pavement construction. Delivery trucks should be covered with tarps or a similar covering used to prevent dust. Trucks and road construction machinery need to be disinfected using good hygiene practices and safe cleaning techniques.

Saudi Arabia is the most populated country that comprises ~50% of the population in the Arabian Peninsula, Coronavirus Cases: 386,782, Deaths: 6,630, Recovered: 375,831 as shown in Table 3 (www.worldometers.info).

Table 3

Demographics and COVID-19 cases/deaths for different countries in Saudi Arabia.

Region	Old Cases	Recovery	Active	Deaths
KSA	386,782	375,831	4,452	6,630,
Najran	6,871	6,717	79	75

7. Microstructure analysis

Fig. 17 shows details of the soil-HPPM mixture microscopic study using scanning electron microscope (SEM). To study the mechanism of strengthening, the nature of cracks and their propagation, as well as the effect of HPPM addition, SEM analysis is performed on samples of soil-HPPM obtained after the unconfined compressive strength test.

The inclusion of HPPM may bridge cracks created in the soil matrix, as shown in **Fig. 17a**. As soil microcracks appear, filling HPPM bridges the distance between the neighboring edges of the microcracks while also improving the microstructure of the soil mass. By contacting with the matrix, the HPPM can reduce the crack width and area as they extend further. When soil mass cracks, the added HPPM forms a three-dimensional platform that connects cracks and transmits distributed stress (as shown in **Fig. 10 b, c**). It can be concluded that the bridging impact is the primary mechanism of HPPM reinforcement (as shown in

Fig. 10 b, c and Fig. 17 b, d, e), and the mechanism is as follows:

Cracks will begin to form and grow during compression load; when the crack hits the HPPM reinforcement, the matrix-HPPM interface starts slicing due to tensile stress vertical to the expected path of the continuing cracks. The tension intensity at the tip of the crack reduces as the continuing crack approaches the interface, reducing and preventing crack spreading (Das et al., 2018 and Xie et al., 2021).

When the HPPM content is higher, the HPPM is dispersed unevenly in soil due to poor workability and mixing. Therefore, these HPPM amounts aggregate to form comparatively weaker points that serve as voids, making them more susceptible to cracking, resulting in a decrease in density, compressive strength and CBR. Moreover, it is clear that failure could happen by the rupture or separation of HPPM in some cases. In conclusion, the results of the microstructure analysis are consistent with those obtained through macro tests that are modified Proctor compaction, California bearing ratio (CBR) and the unconfined compressive tests.

8. Conclusions

This study raises serious inquiries regarding new issues in HPPM management in KSA, due to the COVID-19 pandemic. Following the outbreak of the novel coronavirus, logistical problems arose for HPPM management in KSA, while other environmental, technological, and

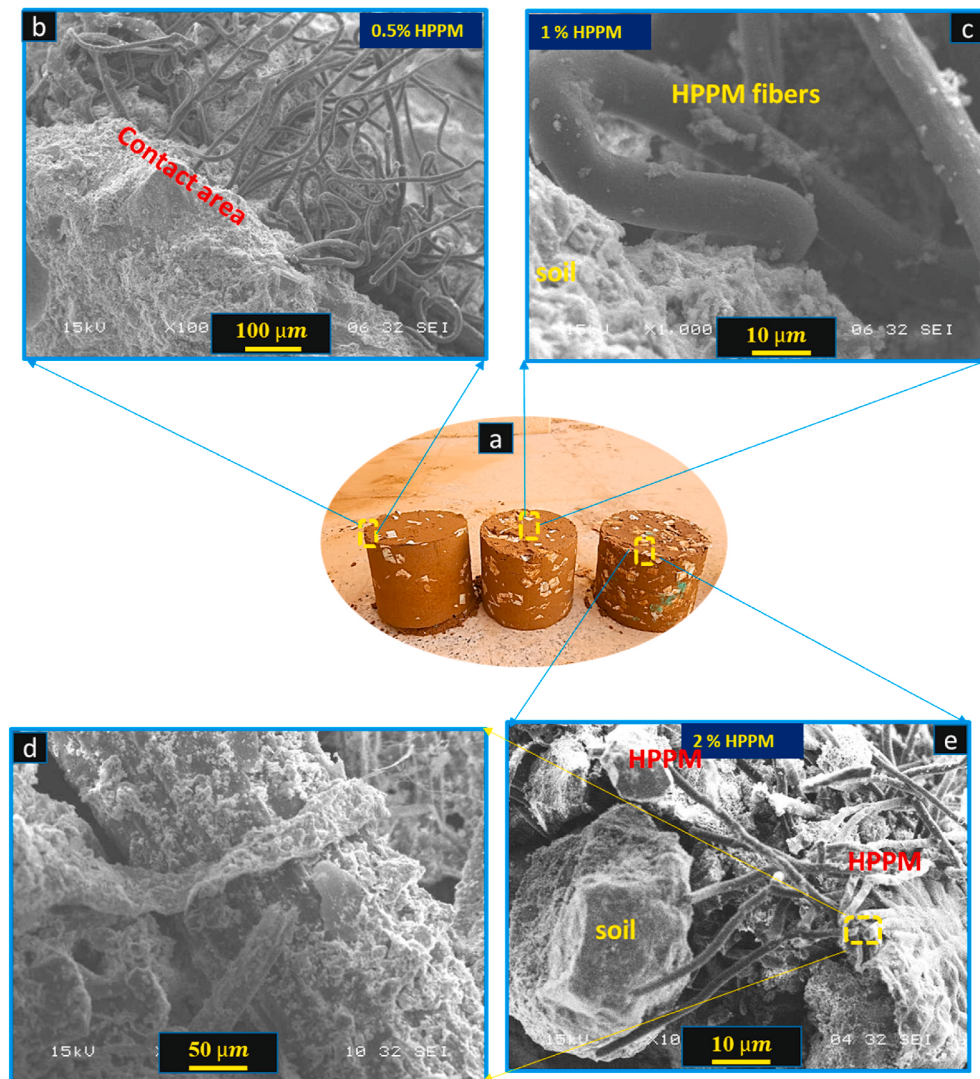


Fig. 17. SEM images of sandy soil with HPPM (a, b, c, and d) cylinders with different percentage of HPPM, 0.5%, 1%, 2% of HPPM fibers.

financial concerns subsided during the COVID-19 crisis. In this regard, government assistance is needed, and public health should take precedence over all other concerns during the COVID-19 pandemic. In most developing countries, including KSA, there is considerable uncertainty about the course of economic recovery. There may be a change in people's habits, which affects HPPM generation and should be discussed in future works. From waste separation and storage guidelines in homes and hospitals to waste collection team safety protocols during the pandemic, significant systemic changes in waste management in KSA are needed. The separation, storage, and recycling of HPPM, including medical waste, from both hospital and non-hospital sources should be emphasized as national priorities.

This paper suggests a new method for minimizing pandemic-related waste in Saudi Arabia by recycling used healthy personal protective materials (HPPM) in enhancing geotechnical engineering of the silty sand soil covering large areas in the Kingdom of Saudi Arabia and the world for using as subbase layer in road pavement structures. From the experimental and numerical results of the current study, the following can be concluded:

- There was a decrease in maximum dry density and an increase in optimum moisture content with increased addition of HPPM percentages due to the low specific gravity and water absorption of HPPM.
- UVP results confirmed the trend of decreasing the maximum dry density with increasing HPPM addition obtained from the modified compaction test in which the UVP decreased with the increase in the HPPM contents as well.
- There was a clear trend in UCS and CBR, suggesting that 0.5 percent of HPPM was the best amount to incorporate into the soil. As the fibers become more closely dispersed, the increase in UCS and CBR tests becomes apparent and satisfy the requirement for using in subbase layer in pavement structures.
- The transformation of stress to polypropylene fibrous enhanced the strength and stiffness of the soil with HPPM by up to 0.5 percent as compared to the reference soil.
- Finite element modeling results indicated the high performance of soil-HPPM mixture as subbase layer under heavy traffic loading in the pavement structure compared to the normal subbase layer in which the vertical displacement reduced by a 11%.
- Soil-HPPM subbase layer enhanced the engineering performance of the total pavement structure and reduced the rutting and fatigue distresses by the bridge-reinforcement action.

Therefore, HPPM can be used as a construction material to create a high-stiffness soil mix and a clean healthy climate.

Finally, people, businesses, factories, and countries must collaborate to improve the care and management of HPPM waste. Consequently, focusing on the most serious causes of HPPM waste and working on them with both political will and public participation is critical. Imbalances in waste management systems must be addressed as a priority for the kingdom of Saudi Arabia to achieve sustainable development and reduce the environmental impacts of wastes. It is also critical to develop strategies and policies to make the region more prosperous, responsible, and environmentally friendly and improve environmental care and respect.

Data availability statement

Data supporting the findings of this study are available from the corresponding author upon reasonable request.

Declaration of competing interest

The authors whose names are listed immediately below certify that they have NO affiliations with or involvement in any organization or entity with any financial interest (such as honoraria; educational grants;

participation in speakers' bureaus; membership, employment, consultancies, stock ownership, or other equity interest; and expert testimony or patent-licensing arrangements), or non-financial interest (such as personal or professional relationships, affiliations, knowledge or beliefs) in the subject matter or materials discussed in this manuscript.

Acknowledgment

The authors would like to express their Gratuities to the Ministry of Education and the deanship of scientific research – Najran University – Kingdom of Saudi Arabia for their financial and Technical support under code number (NU-/SERC/10/533).

References

- ASTM D559/D559M-15, 2015. Standard test methods for wetting and drying compacted soil-cement mixtures. ASTM International. <https://doi.org/10.1520/D0559-D0559M-15>. West Conshohocken, PA. www.astm.org.
- Joint Committee on Powder Diffraction Standards, 1970. Anal. Chem. 42 (11) <https://doi.org/10.1021/ac60293a779>, 81A–81A.
- Abdullah, G.M.S., Al-Abdul Wahhab, H.I., 2015. Evaluation of foamed sulfur asphalt stabilized soils for road applications. Construct. Build. Mater. 88, 149–158. <https://doi.org/10.1016/j.conbuildmat.2015.04.013>.
- Abdullah, G.M.S., Al-Abdul Wahhab, H.I., 2019. Stabilisation of soils with emulsified sulphur asphalt for road applications. Road Mater. Pavement Des. 20 (5) <https://doi.org/10.1080/14680629.2018.1436465>, 2019.
- Al Adili, A., Azzam, R., Spagnoli, G., et al., 2012. Strength of soil reinforced with fiber materials (Papyrus). Soil Mech. Found. Eng. 48, 241–247. <https://doi.org/10.1007/s11204-012-9154-z>.
- Alex, A., 2000. Characterization of unbound granular layers in flexible pavements. Report No. ICAR/502-3, Texas Transportation Institute, and cement-stabilized Shanghai soft clay. Geotech. Remember. 43 (6), 515–523. <http://hdl.handle.net/2152/35440>.
- Astm C597-16, 2016. Standard test method for pulse velocity through concrete. ASTM International. <https://doi.org/10.1520/C0597-16>. West Conshohocken, PA. www.astm.org.
- Astm D1557-12e1, 2012. Standard test methods for laboratory compaction characteristics of soil using modified effort (56,000 ft-lbf/ft³ (2,700 kN-m/m³)). ASTM International. <https://doi.org/10.1520/D1557-12R21>. West Conshohocken, PA. www.astm.org.
- Astm D1883, 16, 2016. Standard test method for California bearing ratio (CBR) of laboratory compacted soils. ASTM International. <https://doi.org/10.1520/D1883-16>. West Conshohocken, PA. www.astm.org.
- Astm D2166/D2166M-16, 2016. Standard test method for unconfined compressive strength of cohesive soil. ASTM International. <https://doi.org/10.1520/D2166-D2166M-16>. West Conshohocken, PA. www.astm.org.
- Astm D422-63(2007) e2, 2007. Standard Test Method for Particle-Size Analysis of Soils (Withdrawn 2016). ASTM International, West Conshohocken, PA. <https://doi.org/10.1520/D0422-63R07E02>.
- ASTM D4318-17e1, 2017. Standard Test Methods for Liquid Limit, Plastic Limit, and Plasticity Index of Soils. ASTM International, West Conshohocken, PA. <https://doi.org/10.1520/D4318-17E01>. ASTM D424-54(1971) Standard Method of Test for Plastic Limit (Withdrawn 1982). www.astm.org.
- Astm D854-14, 2014. Standard test methods for specific gravity of soil solids by water pycnometer. ASTM International. <https://doi.org/10.1520/D0854-14>. West Conshohocken, PA. www.astm.org.
- Bojnourdi, S., SheikhiNarani, S., Abbaspour, M., Ebadi, T., Mir Mohammad Hosseini, S. M., 2020. Hydro-mechanical properties of unreinforced and fibre-reinforced used motor oil (UMO)-contaminated sand-bentonite mixtures. Eng. Geol. 279, 105886. <https://doi.org/10.1016/j.enggeo.2020.105886>.
- Boroujeni, M., Saberian, M., Li, J., 2021. Environmental impacts of COVID-19 on Victoria, Australia, witnessed two waves of coronavirus. Environmental Science and Pollution Research. <https://doi.org/10.1007/s11356-021-12556-y>.
- Chen, M., Shen, S.L., Arulrajah, A., Wu, H.N., Hou, D.W., Xu, Y.S., 2015. Laboratory evaluation on the effectiveness of polypropylene fibres on the strength of fibre-reinforced. Geotext. Geomembranes 43 (6), 515–523. <https://doi.org/10.1016/j.geotexmem.2015.05.004>.
- Das, C.S., Dey, T., Dandapat, R., Mukharjee, B.B., Kumar, J., 2018. Performance evaluation of polypropylene fibre reinforced recycled aggregate concrete. Construct. Build. Mater. 189 (2018), 649–659. <https://doi.org/10.1016/j.conbuildmat.2018.09.036>.
- Doan, H.N., 2020. Medical Face Masks Can Be Reused with Microwave Method: Expert. <https://vietnamnews.vn/society/654072/medical-face-masks-can-be-reused-with-microwave-method-expert.html>.
- Fadare, O.O., Okoffo, E.D., 2020. Covid-19 facemasks: a potential source of microplastic fibers in the environment. Sci. Total Environ. 737, 140279. <https://doi.org/10.1016/j.scitotenv.2020.140279>.
- Fener, M., Kahraman, S., Bay, Y., Gunaydin, O., 2005. Correlations between P-wave velocity and Atterberg limits of cohesive soils. Can. Geotech. J. 42, 673–677.
- Gray, D.H., Ohashi, H., 1983. Mechanics of fiber reinforcement in sand. J. Geotech. Eng. ASCE 109 (3), 335–353. [https://doi.org/10.1061/\(ASCE\)0733-9410\(1983\)109:3\(335\)](https://doi.org/10.1061/(ASCE)0733-9410(1983)109:3(335)).

- Hale, R.C., Song, B., 2020. Single-use plastics and COVID-19: scientific evidence and environmental regulations. *Environ. Sci. Technol.* 54, 7034–7036. <https://doi.org/10.1021/acs.est.0c02269>.
- Henneberry, B., 2020. How surgical masks are made [Online]. Thomas. Net Available: https://www.thomasnet.com/articles/other/how_surgical-masks-are-made/. (Accessed 7 October 2020).
- Jiang, J.Q., 2018. Occurrence of microplastics and its pollution in the environment: a review. *Sustainable Production and Consumption* 13, 16–23. <https://doi.org/10.1016/j.spc.2017.11.003>.
- Kampf, G., Todt, D., Pfaender, S., Steinmann, E., 2020. Persistence of coronaviruses on inanimate surfaces and their inactivation with biocidal agents. *J. Hosp. Infect.* 104 (3), 246–251. <https://doi.org/10.1016/j.jhin.2020.01.022>.
- Leng, Z., Padhan, R.K., Sreeram, A., 2018. Production of a sustainable paving material through chemical recycling of waste PET into crumb rubber modified asphalt. *J. Clean. Prod.* 180, 682–688. <https://doi.org/10.1016/j.jclepro.2018.01.171>, 2018.
- Maher, M.H., Gray, D.H., 1990. Static response of sands reinforced with randomly distributed fibers. *J. Geotech. Eng., ASCE* 116 (11), 1661–1677. [https://doi.org/10.1061/\(ASCE\)0733-9410\(1990\)116:11\(1661\)](https://doi.org/10.1061/(ASCE)0733-9410(1990)116:11(1661)).
- Maher, M.H., Ho, Y.C., 1994. Mechanical properties of kaolinitic fiber soil composite. *J. Geotech. Engineering* 120 (No. 6), 1381–1393. [https://doi.org/10.1061/\(ASCE\)0733-9410\(1994\)120:8\(1381\)](https://doi.org/10.1061/(ASCE)0733-9410(1994)120:8(1381)).
- Mavrokefalidis, D., 2020. Coronavirus face masks ‘could have a devastating effect on the environment’ [Online]. Energy Live Available (Accessed). (Accessed 15 October 2020).
- MolaAbasi, H., Saberian, M., Li, J., 2019. Prediction of compressive and tensile strengths of zeolite-cemented sand using porosity and composition. *Construct. Build. Mater.* 202, 784–795. <https://doi.org/10.1016/j.conbuildmat.2019.01.065>.
- Neto, J.A.B., Gaylarde, C., Beech, I., Bastos, A.C., da Silva Quaresma, V., de Carvalho, D.G., 2019. Microplastics and attached microorganisms in sediments of the Vitória bay estuarine system in SE Brazil. *Ocean Coast Manag.* 169, 247–253. <https://doi.org/10.1016/j.ocecoaman.2018.12.030>.
- Nzediegwu, C., Chang, S.X., 2020. Improper solid waste management increases potential for COVID-19 spread in developing countries. *Resour. Conserv. Recycl.* 161, 104947. <https://doi.org/10.1016/j.resconrec.2020.104947>.
- Perera, S., Arulrajah, A., Wong, Y.C., Horpibulsuk, S., Maghool, F., 2019. Utilizing recycled PET blends with demolition wastes as construction materials. *Construct. Build. Mater.* 221, 200–209. <https://doi.org/10.1016/j.conbuildmat.2019.06.047>.
- Prata, J.C., Silva, A.L.P., da Costa, J.P., Mouneyrac, C., Walker, T.R., Duarte, A.C., Rocha-Santos, T., 2019 Jul 7. Solutions and integrated strategies for the control and mitigation of plastic and microplastic pollution. *Int. J. Environ. Res. Publ. Health* 16 (13), 2411. <https://doi.org/10.3390/ijerph16132411>.
- Prata, J.C., Silva, A.L.P., Walker, T.R., Duarte, A.C., Rocha-Santos, T., 2020. COVID-19 pandemic repercussions on the use and management of plastics. *Environ. Sci. Technol.* 54, 7760–7765. <https://doi.org/10.1021/acs.est.0c02178>.
- Qu, J., Zhu, H., 2021. Function of palm fiber in stabilization of alluvial clayey soil in Yangtze River estuary. *Journal of Renewable Materials* 9, 4. <https://doi.org/10.32604/jrm.2021.013816>, 2021.
- Rao, G.V., Balan, K., 2000. Coir Geotextiles-Emerging Trends. Kerala State Coir Corporation Limited, Alappuzha, Kerala.
- Roberts, K.P., Cressida, B., Kolstoe, S., Steve, F., 2020. Coronavirus face masks: an environmental disaster that might last generations [Online]. the conversation (Accessed). <https://theconversation.com/coronavirus-face-masks-anenvironmental-disaster-that-might-last-generations-144328>. (Accessed 7 October 2020).
- Rowan, N.J., Laffey, J.G., 2020. Unlocking the surge in demand for personal and protective equipment (PPE) and improvised face coverings arising from coronavirus disease (COVID-19) pandemicImplications for efficacy, re-use and sustainable waste management. *Sci. Total Environ.* 752, 142259. <https://doi.org/10.1016/j.scitotenv.2020.142259>.
- Saberian, M., Li, J., Kilmartin-Lynch, S., Boroujeni, M., 2021. Repurposing of COVID-19 single-use face masks for pavements base/subbase. *Sci. Total Environ.* 769, 145527. <https://doi.org/10.1016/j.scitotenv.2021.145527>, 2021.
- Sangkham, S., 2020. Face mask and medical waste disposal during the novel COVID-19 pandemic in Asia. *Case Studies in Chemical and Environmental Engineering* 2, 100052. <https://doi.org/10.1016/j.cscee.2020.100052>.
- Sudhakaran, S., Sharma, A., Kolathayar, S., 2018. Soil stabilization using bottom ash and areca fiber: experimental investigations and reliability analysis. *J. Mater. Civ. Eng.* 30 (8), 04018169 [https://doi.org/10.1061/\(ASCE\)MT.1943-5533.0002326](https://doi.org/10.1061/(ASCE)MT.1943-5533.0002326), 2018.
- Tang, C., Shi, B., Gao, W., Chen, F., Cai, Y., 2007. Strength and mechanical behavior of short polypropylene fiber reinforced and cement stabilized clayey soil. *Geotext. Geomembranes* 25, 194–202. <https://doi.org/10.1016/j.geotexmem.2006.11.002>, 2007.
- Thomas, G.P., 2012. Recycling of polypropylene (PP) [Online]. AZO Cleantech. Available: [https://www.azocleantech.com/article.aspx?ArticleID=240#:%7E-,text=While%20PP%20is%20easily%20among,slowly%20over%2020%2D30%20](https://www.azocleantech.com/article.aspx?ArticleID=240#:%7E:text=While%20PP%20is%20easily%20among,slowly%20over%2020%2D30%20).
- Tomar, A., Sharma, T., Singh, S., 2020. Strength properties and durability of clay soil treated with mixture of nano-silica and polypropylene fiber. *Materials Today Proceedings* 26 (3), 3449–3457. <https://doi.org/10.1016/j.matepro.2019.12.239>.
- Wahab, R.M., Heckel, G.B., Qurna, H.H.A., 1997. Total and effective strength parameters of compacted fiber reinforced soils. *Proc. 14th Int. Conf. on Soil Mechanics and Foundation Engineering* 1, 423–426. <https://doi.org/10.1007/s11204-012-9154-z>, Hamburg, Germany.
- Who, 2020. Rational Use of Personal Protective Equipment (PPE) for Coronavirus Disease (COVID-19).
- World Health Organization, Who. WHO, 2020b. Shortage of Personal Protective Equipment Endangering Health Workers Worldwide. The World Health Organization (WHO). https://apps.who.int/iris/bitstream/handle/10665/331215/WHO-2019-n-Cov-ICPPPE_use-2020.1-eng.pdf. (Accessed 9 August 2020). <https://www.who.int/newsroom/detail/03-03-2020-shortage-of-personal-protective-equipment>.
- Worldometers. info.coronavirus/country/saudi-arabia.
- Wu, Y., Li, Y., Niu, B., 2014. Assessment of the mechanical properties of sisal fiber-reinforced silty clay using triaxial shear tests. *Sci. World J.* 2014, 9. <https://doi.org/10.1155/2014/436231>. Article ID 436231.
- Xiang, Y., Song, Q., Gu, W., 2020. Decontamination of surgical face masks and N95 respirators by dry heat pasteurization for one hour at 70°C. *Am. J. Infect. Contr.* 48 (8), 880–882. <https://doi.org/10.1016/j.ajic.2020.05.026>.
- Xie, Jing, Kou, Shi-cong, Ma, Hongyan, Long, Wu-Jian, Wang, Yaocheng, Ye, Tao-Hua, 2021. Advances on properties of fiber reinforced recycled aggregate concrete: experiments and models. *Construct. Build. Mater.* 277, 122345. <https://doi.org/10.1016/j.conbuildmat.2021.122345>.
- Yaghoubi, E., Arulrajah, A., Wong, Y.C., Horpibulsuk, S., 2017. Stiffness properties of recycled concrete aggregate with polyethylene plastic granules in unbound pavement applications. *J. Mater. Civ. Eng.* 29 (4) [https://doi.org/10.1061/\(ASCE\)MT.1943-5533.0001821](https://doi.org/10.1061/(ASCE)MT.1943-5533.0001821), 04016271 (1-7).
- Zhang, J., Ding, L.e., Li, F., Peng, J., 2020. Recycled aggregates from construction and demolition wastes as alternative filling materials for highway subgrades in China. *J. Clean. Prod.* 255 (2020), 120223. <https://doi.org/10.1016/j.jclepro.2020.120223>.
- Zhang, J., Li, C., Ding, L., Li, J., 2021a. Performance evaluation of cement stabilized recycled mixture with recycled concrete aggregate and crushed brick. *Construct. Build. Mater.* 296 (2021), 123596.
- Zhang, J., Zhang, A., Huang, C., Yu, H., Zhou, C., 2021b. Characterising the resilient behaviour of pavement subgrade with construction and demolition waste under Freeze-Thaw cycles. *J. Clean. Prod.* 300 (2021), 126702. <https://doi.org/10.1016/j.jclepro.2021.126702>.